Hyphal Branching during Arbuscule Development Requires *Reduced Arbuscular Mycorrhiza1*[1][OPEN]

Hee-Jin Park, Daniela S. Floss, Veronique Levesque-Tremblay, Armando Bravo, and Maria J. Harrison*

Boyce Thompson Institute for Plant Research, Ithaca, New York 14853

ORCID ID: 0000-0001-8716-1875 (M.J.H.).

During arbuscular mycorrhizal symbiosis, arbuscule development in the root cortical cell and simultaneous deposition of the plant periarbuscular membrane generate the interface for symbiotic nutrient exchange. The transcriptional changes that accompany arbuscule development are extensive and well documented. By contrast, the transcriptional regulators that control these programs are largely unknown. Here, we provide a detailed characterization of an insertion allele of *Medicago truncatula* Reduced Arbuscular Mycorrhiza1 (RAM1), *ram1-3*, which reveals that RAM1 is not necessary to enable hyphopodium formation or hyphal entry into the root but is essential to support arbuscule branching. In *ram1-3*, arbuscules consist only of the arbuscule trunk and in some cases, a few initial thick hyphal branches. *ram1-3* is also insensitive to phosphate-mediated regulation of the symbiosis. Transcript analysis of *ram1-3* and ectopic expression of *RAM1* indicate that RAM1 regulates expression of *EXO70I* and *Stunted Arbuscule*, two genes whose loss of function impacts arbuscule branching. Furthermore, RAM1 regulates expression of a transcription factor *Required for Arbuscule Development* (*RAD1*). RAD1 is also required for arbuscular mycorrhizal symbiosis, and *rad1* mutants show reduced colonization. *RAM1* itself is induced in colonized root cortical cells, and expression of *RAM1* and *RAD1* is modulated by DELLAs. Thus, the data suggest that DELLAs regulate arbuscule development through modulation of RAM1 and RAD1 and that the precise transcriptional control essential to place proteins in the periarbuscular membrane is controlled, at least in part, by RAM1.

The symbiotic association of plants and arbuscular mycorrhizal fungi, known as arbuscular mycorrhiza (AM), is widespread in terrestrial ecosystems. In this association, the fungal symbiont delivers mineral nutrients to the plant in return for carbon, and as a consequence, the symbiosis has a major impact on plant productivity (Smith and Read, 2008). AM is an endosymbiosis, and the fungus lives within the root cortical cells, where it develops differentiated hyphae called arbuscules. To support arbuscule development, the cortical cell undergoes considerable reorganization, including development of a new membrane-bound apoplastic compartment in which the arbuscule resides. This symbiotic interface is the site of nutrient exchange between the symbionts and therefore, critical for symbiotic function (Feddermann et al., 2010; Pumplin et al., 2010; Murray et al., 2011; Smith and Smith, 2011).

Development of AM symbiosis is initiated with signal exchange between the symbionts (Akiyama et al., 2005; Besserer et al., 2006; Maillet et al., 2011; Kretzschmar et al., 2012; Wang et al., 2012; Genre et al., 2013) and the activation of a plant signaling pathway referred to as the common symbiosis signaling pathway. In legumes, this pathway is essential for symbiosis with rhizobia as well as AM fungi, and several proteins that constitute the shared core of the pathway have been identified (Oldroyd, 2013). Among these shared components is a transcription factor (TF) called CYCLOPs (Yano et al., 2008; Singh et al., 2014), which is required for arbuscule development. There are extensive transcriptional changes in the root cortex associated with arbuscule development (Gaude et al., 2012; Hogekamp and Küster, 2013), but currently, genes regulated by CYCLOPS that enable arbuscule development are unknown.

Several plant genes required for arbuscule development and/or function have been identified, including Vapyrin (Feddermann et al., 2010; Pumplin et al., 2010; Murray et al., 2011), two Vesicle-Associated Membrane Proteins (Ivanov et al., 2012), EXO70I (Zhang et al., 2015), proteases (Takeda et al., 2009; Rech et al., 2013),

[1] This work was supported by the Office of Science (Biological and Environmental Research), U.S. Department of Energy (grant no. DE FG02–08ER64628), the National Science Foundation (grant nos. IOS–1127155, IOS–1237993 and DBI–0618969 [instrumentation grant for microscopes in the Boyce Thompson Institute for Plant Research, Plant Cell Imaging Center]). *Medicago truncatula* insertion mutant lines were obtained from the Samuel Roberts Noble Foundation.

* Address correspondence to mjh78@cornell.edu.

The author responsible for distribution of materials integral to the findings presented in this article in accordance with the policy described in the Instructions for Authors (www.plantphysiol.org) is: Maria J. Harrison (mjh78@cornell.edu).

H.-J.P. and M.J.H. conceived the experiments; H.-J.P. performed the majority of the research, generated the figures, and contributed to the writing of "Methods" and "Results"; D.S.F. contributed the DELLA data; V.L.-T. performed the qRT-PCR analyses; A.B. contributed part of the RAD1 phenotype data and phylogenetic analysis; M.J.H. wrote the article.

[OPEN] Articles can be viewed without a subscription.

www.plantphysiol.org/cgi/doi/10.1104/pp.15.01155

a proton ATPase (Krajinski et al., 2014; Wang et al., 2014), ATP-binding cassette (ABC) transporters, Stunted Arbuscule (STR) and STR2 (Zhang et al., 2010; Gutjahr et al., 2012), and phosphate transporters (Javot et al., 2007; Yang et al., 2012; Xie et al., 2013). Some of these genes are expressed only during AM symbiosis, whereas others have broader expression patterns. In addition, some are expressed exclusively in cells containing arbuscules. The variety of expression patterns points to complex transcriptional and possibly posttranscriptional regulation (Devers et al., 2011). Furthermore, trafficking of the symbiotic phosphate transporters and ABC transporters to the periarbuscular membrane requires gene expression coincident with arbuscule branching (Pumplin et al., 2012). Thus, transcriptional control is not only essential to ensure expression of symbiosis-specific genes, but in the cortical cells, precise timing of gene expression ensures the correct protein composition of the periarbuscular membrane (Pumplin et al., 2012).

So far, transcription factors required for AM symbiosis include CYCLOPS (Yano et al., 2008), DELLAs (Floss et al., 2013; Foo et al., 2013; Yu et al., 2014; Takeda et al., 2015), Reduced Arbuscular Mycorrhiza1 (RAM1; Gobbato et al., 2012; Rich et al., 2015; Xue et al., 2015), Required for Arbuscule Development1 (RAD1; Xue et al., 2015), MtERF1 (Devers et al., 2013), and DELLA-Interacting Protein1 (DIP1; Yu et al., 2014). Among these transcriptional regulators, DELLAs, RAM1, RAD1, and DIP1 belong to the GRAS (for GA_3 insensitive [GAI], Repressor of GAI [RGA], and Scarecrow [SCR]) family, a large, plant-specific gene family with members that regulate transcription and influence several aspects of plant development, including root development (Bolle, 2004). DELLAs were identified originally as repressors of GA_3 signaling but have emerged as major transcriptional regulators that mediate cross talk between hormone, development, and defense signaling pathways through interactions with a wide range of TFs (Davière and Achard, 2013). *Medicago truncatula* and pea (*Pisum sativum*) *della1della2* double mutants are unable to support arbuscule development (Floss et al., 2013; Foo et al., 2013) and show a symbiosis phenotype similar to that of *cyclops*. In contrast, in the rice (*Oryza sativa*) *della* mutant, *slender* (*slr*), the symbiosis fails before arbuscule development at the epidermal stage (Yu et al., 2014). Rice has only one DELLA gene, which possibly accounts for this difference. Ectopic expression of a dominant DELLA protein in *cyclops* enables arbuscule development, which suggests that DELLAs modulate symbiosis by acting on the symbiosis signaling pathway downstream of CYCLOPS, likely regulating other, as yet unknown TFs (Floss et al., 2013).

In *M. truncatula*, RAM1 was reported to be necessary to enable hyphopodium formation and directly regulates RAM2, a glycerol-3-P acyltransferase (Gobbato et al., 2012). RAM2 is required for the biosynthesis of the cutin monomer signal that induces hyphophodium formation (Gobbato et al., 2012; Wang et al., 2012). However, subsequently, it was noted that arbuscules in *ram1* were small, suggesting a potential role for RAM1 in arbuscule development (Gobbato et al., 2013). Recent analyses of *ram1* mutants in *Lotus japonicus* and *Petunia hybrida* show that RAM1 is required to support wild-type arbuscule development (Rich et al., 2015; Xue et al., 2015). In *L. japonicus*, a second GRAS factor RAD1 interacts with RAM1, and *rad1* mutants showed a high proportion of small, degenerated arbuscules, suggesting a requirement for RAD1 in maintenance of the symbiosis (Xue et al., 2015). Rice DIP1, identified as an interactor of SLR, also interacts with RAM1, and DIP1 RNA interference lines showed a quantitative reduction in symbiotic development (Yu et al., 2014). Thus, several aspects of AM symbiosis are influenced by GRAS factors, which likely operate in complexes, potentially with a range of partners, such as has been shown for GRAS factors regulating other developmental processes (Cui and Benfey, 2009; Hirsch et al., 2009; Zhang et al., 2011). In addition to the GRAS factors, many other TFs are induced during symbiosis, including ERF1, an Apetala2 domain factor. Downregulation of ERF1 resulted in a quantitative decrease in symbiosis (Devers et al., 2013). Currently, other than RAM2, the genes regulated by these TFs are unknown.

During a reverse genetic screen of TFs expressed in cells hosting arbuscules, we characterized the AM phenotype of a third allele of *RAM1*, *ram1-3*. Our data indicate that RAM1 is essential for a plant cellular program that enables arbuscule branching and modulates expression of *EXO70I* and *STR*, two genes essential for the branching phase of arbuscule development.

RESULTS

ram 1-3 Is Unable to Support Arbuscule Branching

From a search for TFs that showed transcriptional induction during AM symbiosis, we identified RAM1 (Gobbato et al., 2012), a member of the GRAS family (Fig. 1A). Analysis of *M. truncatula* roots expressing two *RAM1pro-β-glucuronidase* (*UidA*) fusions revealed that 2 kb or 800 bp of putative *RAM1* promoter directed transcription in the cortex in colonized regions of the root (Supplemental Fig. S1, A–C) and to a lesser extent, noncolonized lateral roots of a symbiotic root system. Additionally, young lateral roots of mock-inoculated root systems also showed GUS staining, although *RAM1* transcripts were not detectable in mock-inoculated roots by quantitative reverse transcription (qRT)-PCR (Fig. 1A; Supplemental Fig. S1, D and E).

To address the function of *RAM1*, we obtained a *M. truncatula* line (NF5445) with a transposable element of *Nicotiana tabacum* cell type1 (*Tnt1*) insertion between nucleotides 1,318 and 1,319 of Medtr7g027190, which truncates the protein after amino acid 310 (Supplemental Fig. S2). Previously, two mutant alleles of *RAM1* had been reported: *ram1-1*, which has a 71-kb deletion that includes the *RAM1* gene, and *ram1-2*, which contains a *Tnt1* insertion that truncates the protein after amino acid 649 (Gobbato et al., 2012; Supplemental Fig. S2).

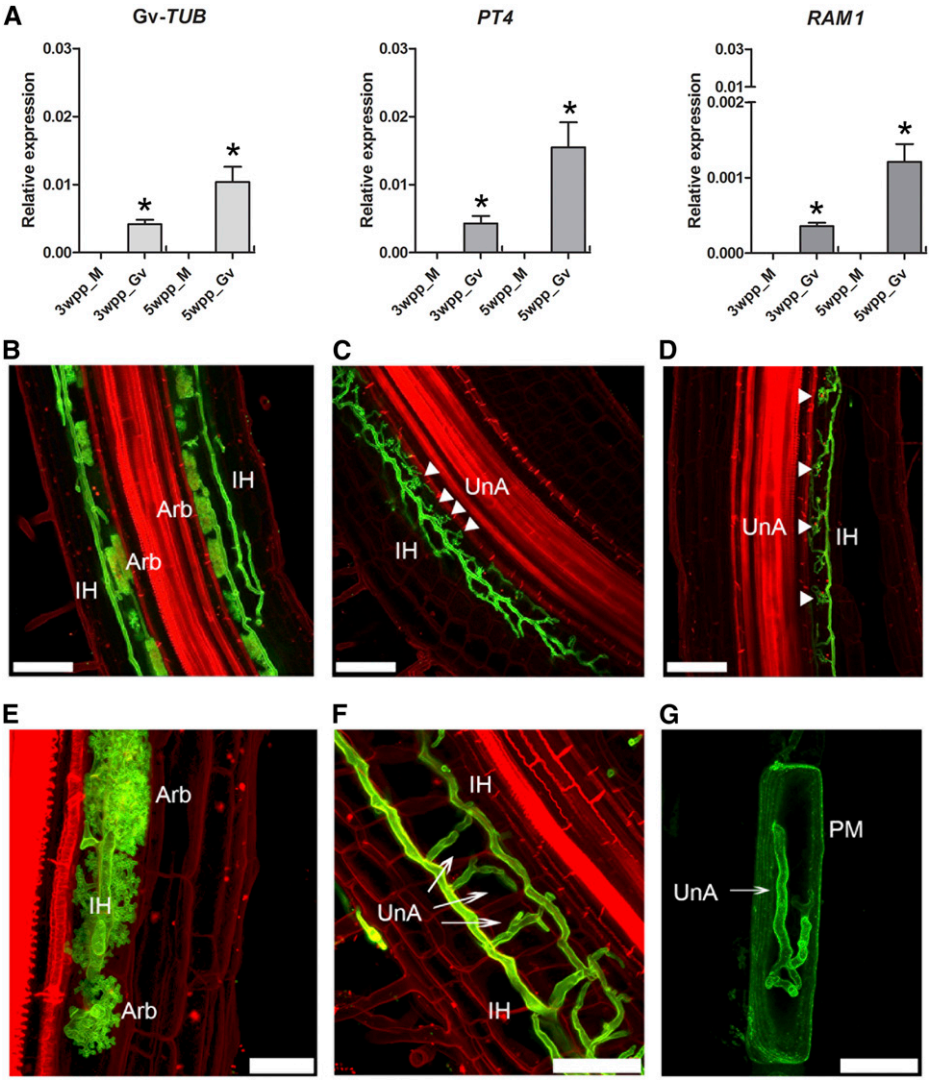

Figure 1. *RAM1* expression and the mycorrhizal phenotype of *ram1-3*. A, Relative expression of *RAM1*, *G. versiforme* α-*tubulin* (*GvTUB*), and *PT4* in wild-type *M. truncatula* (A17) roots either mock inoculated (M) or colonized with *G. versiforme* at 3 and 5 wpp. Transcript levels are relative to *elongation factor1α*. Error bars show SEM ($n = 3$). *, Significant differences between the mock-inoculated control (M) and colonized (*G. versiforme*) roots (Student's *t* test; $P < 0.05$). B to F, Confocal microscope images of an *M. truncatula* wild-type segregant (B and E) and *ram1-3* (C, D, and F) roots colonized with *G. versiforme*. The roots at 8 dpi were stained with Alexa Fluor 488 WGA and propidium iodide. The images in E and F are projections of 30 and 20 optical sections on the *z* axis, respectively, taken at 2-μm intervals. G, A confocal microscope image of a cortical cell from an *ram1-3* root expressing *BCP1*:*MtPT1-GFP*. Labeling of the arbuscule trunk indicates that the trunk is surrounded by a membrane. The image is a projection of 15 optical sections on the *z* axis taken at 1-μm intervals. White arrowheads point to undeveloped arbuscules. White arrows point to arbuscule trunks. Arb, Arbuscule; IH, intercellular hyphae; PM, plasma membrane; UnA, undeveloped arbuscules. Bars = 75 μm (B–D), 25 μm (E and G), and 10 μm (F).

Consequently, we labeled our insertion allele (NF5445) *ram1-3*. The mycorrhizal phenotype reported for *ram1-1* included a defect in hyphopodium formation and substantially reduced colonization but wild-type arbuscules, whereas *ram1-2* showed small, undeveloped arbuscules (Gobbato et al., 2012, 2013). Recent reports of *ram1* mutants of *L. japonicus* and *P. hybrida* noted low colonization and the presence of malformed arbuscules (Rich et al., 2015; Xue et al., 2015).

We evaluated the mycorrhizal phenotype of *ram1-3* at 2 to 8 d postinoculation (dpi) with *Glomus versiforme* spores in a double-cone inoculation system (Lopez-Meyer and Harrison, 2006) and also, 3 and 5 weeks postplanting (wpp) into substrate-containing spores. A microscopic evaluation of the colonized roots revealed obvious differences in fungal development in the root cortex of *ram1-3* relative to the wild type (Fig. 1, B–F). In *ram1-3*, intracellular hyphae, which we inferred to be arbuscule trunks, were present in the inner cortical cells, but arbuscule branches were either absent or limited to one or two thick branches. The fine branches, typical of mature arbuscules, were absent (Fig. 1, C, D, and F). In contrast, infection units with fully branched arbuscules were present in wild-type roots (Fig. 1, B and E). This phenotype was further verified by imaging *ram1-3* roots expressing $BCP1_{pro}$:*PT1-GFP*, which labels the plasma membrane and periarbuscular membrane of colonized cortical cells (Pumplin et al., 2012). In *ram1-3*, intracellular hyphae, sometimes coiled and with occasional bifurcations, were visible in the cells, but highly branched arbuscules were never observed (Fig. 1G).

Fungal structures in *ram1-3* were quantified and compared with those in a wild-type segregant from the *ram1-3* population and the parental line, R108 (Fig. 2). At 2, 4, and 6 dpi, the total number of infection events in which the fungus had successfully penetrated the roots and the number of hyphopodia that had not penetrated the root did not differ between *ram1-3* and wild-type controls (Fig. 2, A–C). In contrast, the number of infection units that contain only intercellular hyphae was slightly higher in *ram1-3* relative to the controls. At 4 and 6 dpi, most infection units in wild-type roots

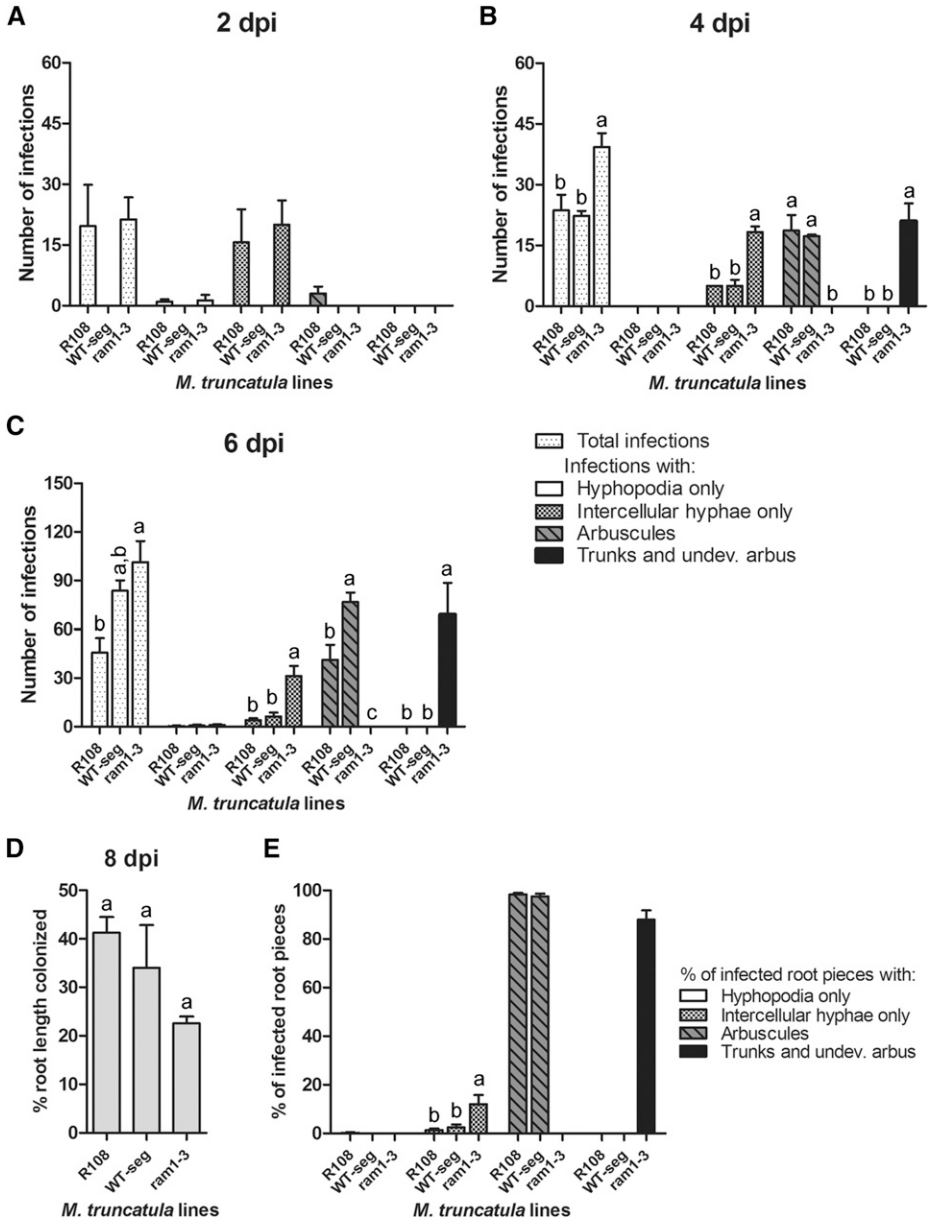

Figure 2. Mutation of RAM1 does not alter the initial infection by *G. versiforme*. A to E, Quantitation of total infection units, hyphopodia, infection units with only intercellular hyphae, infection units with arbuscules, and infection units with arbuscule trunks/undeveloped arbuscules in the wild type (R108), *ram1-3*, and a wild-type segregant (WT-seg) at 2, 4, 6, and 8 dpi in a double-cone assay system. For each line, the data are the means of three biological replicate cones, each containing two plants. Data are averages ± SEM ($n = 3$). Different letters indicate significant differences between the lines in each group of infection phenotypes (all pairs; Tukey's HSD mean-separation test; $P < 0.01$ in B and $P < 0.05$ in C–E). At 2 to 6 dpi, the data shown are the numbers of infections. At 8 dpi, the data shown are percentage of infected root pieces, because the total number of infections was too high to count.

contained fully branched arbuscules, whereas infection units in *ram1-3* contained thick intracellular hyphae, with minimal branching, designated as arbuscule trunks/undeveloped arbuscules (Fig. 2, B and C). The same phenotype was apparent at 8 dpi (Fig. 2, D and E) and also, 3 and 5 wpp (Fig. 3), indicating that mature arbuscules do not develop, even after extensive cocultivation. At these time points, it was not feasible to count the absolute number of infection units, and so, roots were analyzed by the gridline intersect method to obtain the percentage of colonized root length (McGonigle et al., 1990). At 3 and 5 wpp, 18% to 25% of the *ram1-3* root length was colonized. This was significantly lower than the two wild types, where the fungus had proliferated to colonize approximately 70% to 80% of the root length (Fig. 3). Differences in colonized root length in the wild type and *ram1-3* were magnified over time, because colonization progressed in the wild type but not *ram1-3*. This phenotype was seen consistently in independent experiments (Supplemental Figs. S3 and S4).

Because the phenotype reported originally for *ram1-1* (Gobbato et al., 2012) differed substantially from the one that we observed for *ram1-3*, we carried out a side by side comparison of *ram1-3* and *ram1-1* in our growth conditions. The two alleles are in different genetic backgrounds, and consequently, controls included A17, R108, and a wild-type segregant from the *ram1-3* population. At 3 wpp into substrate containing *G. versiforme* spores, *ram1-1* and *ram1-3* showed similar levels of colonization, and both differed significantly from the wild-type controls (Supplemental Fig. S5A). An analysis of the infection phenotype revealed no significant

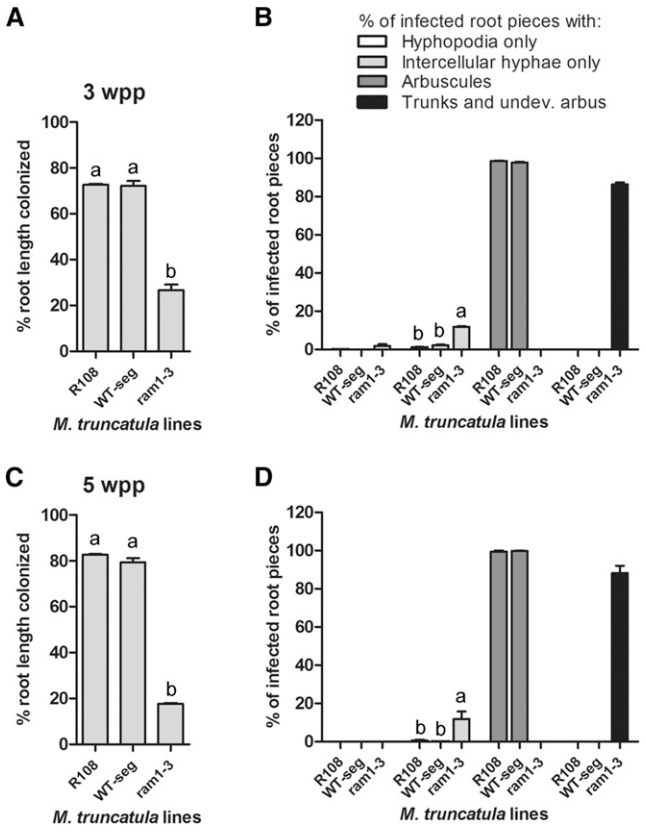

Figure 3. AM symbiosis is not maintained in *ram1-3*, and colonization levels decline over time. A and C show the total percentages of colonized root length, whereas B and D show the percentages of infected root pieces containing hyphopodia, intercellular hyphae only, arbuscules, and arbuscule trunks/undeveloped arbuscules in the wild type (R108), *ram1-3*, and a wild-type segregant (WT-seg) from the *ram1-3* backcrossed population colonized with *G. versiforme* at 3 and 5 wpp into inoculum. Error bars show SEM ($n = 3$). Different letters indicate significant differences between the *M. truncatula* lines in each group of infection phenotypes (all pairs; Tukey's HSD mean-separation test; $P < 0.01$).

differences between *ram1-1* and *ram1-3*, and both mutants showed cortical infections with arbuscule trunks and an absence of fully developed arbuscules (Supplemental Fig. S5, B and C). In this experiment, differences in the number of infections with intercellular hyphae only did not differ between the mutants and the wild type.

To ensure that the *ram1-3* phenotype that we observed is indeed caused by a defect in Medtr7g027190, we carried out a cosegregation analysis and also complemented the *ram1-3* with a wild-type copy of Medtr7g027190. Both analyses indicate that the arbuscule branching defect observed in *ram1-3* is the result of loss of function of Medtr7g027190 (Supplemental Fig. S6). Thus, in these conditions, we do not find evidence to support a role for *RAM1* in hyphal penetration into cells but instead, conclude that it is essential to enable arbuscule development and more specifically, arbuscule branching.

Fungal Morphology in *ram1-3* Roots Is Not Affected by the Nutritional Status of the Plant, But *ram1-3* Is Insensitive to Phosphate-Mediated Suppression of Colonization

Because a previous study indicated that AM fungi were unable to form hyphopodia on *ram1-1* and consequently, impaired in hyphal entry into the root (Gobbato et al., 2012), we questioned whether differences in the nutrient conditions of our experiments might alter the mycorrhizal phenotype and reveal a defect in hyphopodium development. It is well documented that the nutritional status of the plant influences fungal development within the roots (Schwab et al., 1983; Amijee et al., 1989; Baath and Spokes, 1989; Koide and Li, 1990), and in some mutants, nutrient status causes a major phenotypic change (Javot et al., 2011). Consequently, we assessed the mycorrhizal phenotype of *ram1-3* during growth in three different phosphorus (P) and nitrogen (N) regimes. These treatments did not alter the morphology of colonization in *ram1-3* or the wild type (Fig. 4A). However, fertilization with 2 mM P and 7.5 mM N resulted in a decrease in colonization in R108 and the wild-type segregant but did not alter colonization levels in *ram1-3* (Fig. 4B). Currently, the mechanisms by which plant nutrient status regulates colonization levels are unknown. These data suggest that RAM1 may be involved in this process possibly by influencing expression of genes that regulate colonization. Alternatively, it is possible that nutrient-mediated regulation of the symbiosis occurs only on a fully developed mycorrhiza with intact arbuscules and therefore, does not occur in *ram1-3*.

Gene Expression in *ram1-3* Is Consistent with the Failure to Develop Arbuscules

Gene expression in noncolonized *ram1-3* roots and *ram1-3* colonized with *G. versiforme* was compared with those of a wild-type segregant control. *G. versiforme* *α-tubulin* transcript levels were 4-fold lower in *ram1-3* relative to the wild-type segregant, which correlates with lower colonization in *ram1-3* (Fig. 5, A and B). Consistent with the severe arbuscule development phenotype, transcripts of genes whose expression is associated with arbuscule development or function were reduced substantially in *ram1-3* relative to the wild-type segregant control. *Lectin5* (Frenzel et al., 2005) and *MtPT4* (Harrison et al., 2002) transcripts were undetected (Fig. 5, C and D), whereas *STR* (Zhang et al., 2010), *EXO70I* (Zhang et al., 2015), and *Vapyrin* (Pumplin et al., 2010; Murray et al., 2011), each of which is required for arbuscule development, showed basal levels of expression in *ram1-3* colonized roots (Fig. 5, E–G). Likewise, *Blue Copper Binding Protein1* (*BCP1;* Hohnjec et al., 2005; Pumplin and Harrison, 2009), *Serine carboxypeptidase1* (Liu et al., 2003), *Ammonium transporter2;4* (*AMT2;4*), and *AMT2;5* (Breuillin-Sessoms et al., 2015) transcripts also remained at basal levels in *ram1-3* (Fig. 5, H–K). *RAM2*, a verified downstream target of *RAM1*

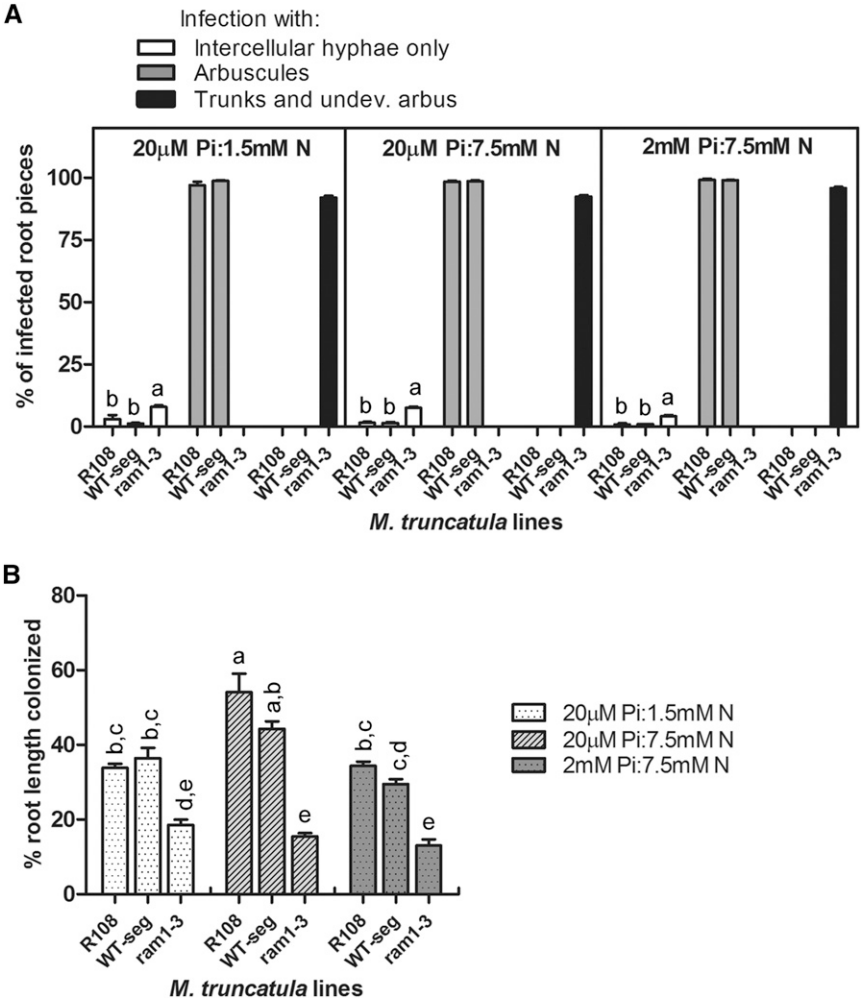

Figure 4. Nutrient treatments do not alter the morphology or levels of colonization in *ram1-3*. The percentages of infected root pieces containing hyphopodia, intercellular hyphae only, arbuscules, and arbuscule trunks/undeveloped arbuscules (A) and the percentages of colonized root length in the wild type (R108), *ram1-3*, and a wild-type segregant (WT-seg) from the *ram1-3* backcrossed population colonized with *G. versiforme* at 3 wpp in three different nutrient regimes. Data are the means of three biological replicates, and error bars indicate SEM. Different letters indicate significant differences between the lines (ANOVA and Tukey's HSD mean-separation test; $P < 0.05$ in 20 μM Pi:1.5 mM N treatment in A; $P < 0.01$ in the two other treatments in A; and $P < 0.05$ in B).

(Wang et al., 2012), was not expressed in *ram1-3* plants (Fig. 5L). We also examined the expression of several other members of the GRAS TF family, including an AM-induced GRAS factor Medtr3g022830 (*TF80*) and the two closest homologs of RAM1, Medtr4g104020 (*RAD1*) and Medtr8g442410 (*TF124*; Supplemental Fig. S7; Supplemental Data Set S1). After colonization, *RAD1* and *TF80* showed transcriptional induction in the wild-type segregant but not in *ram1-3* (Fig. 5, M and N). In contrast, *TF124* is expressed constitutively in both *ram1-3* and the wild-type segregant (Fig. 5O). Nodulation Signaling Pathway1 (NSP1) and NSP2, two GRAS factors that regulate strigolactone biosynthesis (Liu et al., 2011) and influence development of AM in a quantitative manner (Delaux et al., 2013; Hofferek et al., 2014), were likewise not differentially expressed in *ram1-3* (Fig. 5, P and Q). As reported previously, *DELLA* transcripts were not induced during AM symbiosis (Floss et al., 2013), and this was also the case in *ram1-3* (Fig. 5, R–T). Gene expression in control and colonized *ram1-1* roots followed the same pattern as observed in *ram1-3* (Supplemental Fig. S8).

Overexpression of *RAM1* Results in Increases in *RAM2*, *EXO70I*, *STR*, and *RAD1* Transcripts

The differential gene expression observed in *ram1-3* could be a secondary consequence of incomplete arbuscule development, or alternatively, these genes might be regulated by RAM1. To identify genes potentially regulated by RAM1, we generated transgenic roots overexpressing *RAM1* to levels 100-fold higher than the vector controls and assayed expression of possible RAM1 target genes in the absence of symbiosis (Fig. 6). Transcript levels of four genes, *STR*, *EXO70I*, *RAD1*, and *RAM2*, showed small but significant increases in mock-inoculated roots overexpressing *RAM1* relative to a vector control, whereas *TF80* and *Vapyrin* transcripts showed no change; *TF124* transcripts decreased. *RAM2* gene expression is regulated by RAM1 (Gobbato et al., 2012), whereas regulation of the other genes has not been reported previously. *STR* and *EXO70I* are both required to enable arbuscule development, and in *str* and *exo70i* mutants, arbuscule branching fails very early in the developmental process (Zhang et al., 2010, 2015). Their phenotypes are consistent with

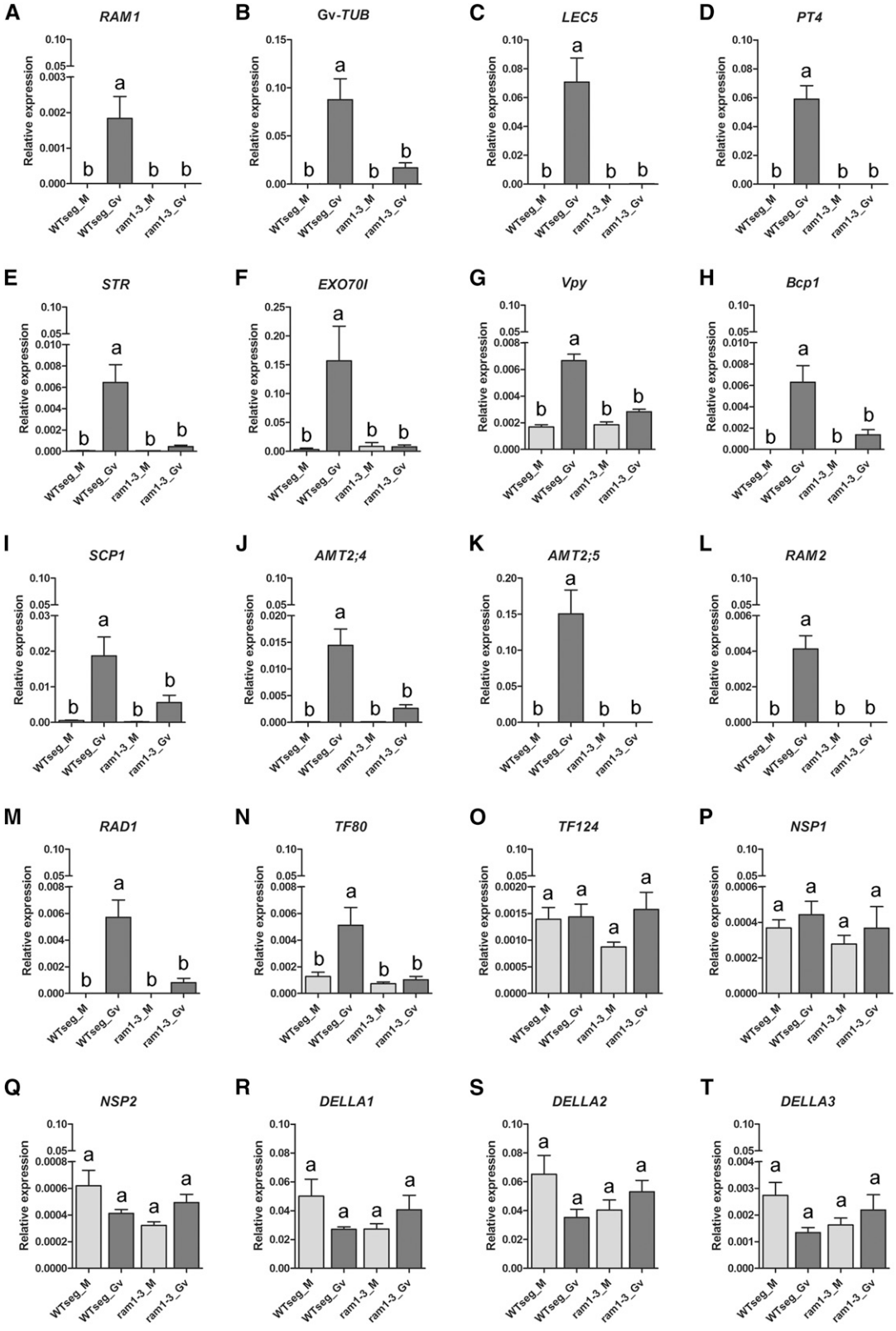

Figure 5. Gene expression in *ram1-3*. Gene expression in *ram1-3* and a wild-type segregant (WTseg) from the *ram1-3* population mock inoculated (M) or colonized with *G. versiforme* at 3 wpp. Transcripts levels are relative to *M. truncatula elongation factor1α*. Different letters indicate significant differences between the lines (all pairs; Tukey's HSD mean-separation test). Error bars are SEM ($n = 4$; $P < 0.01$ in A–F, H, and J–M; and $P < 0.05$ in G, I, and N–T).

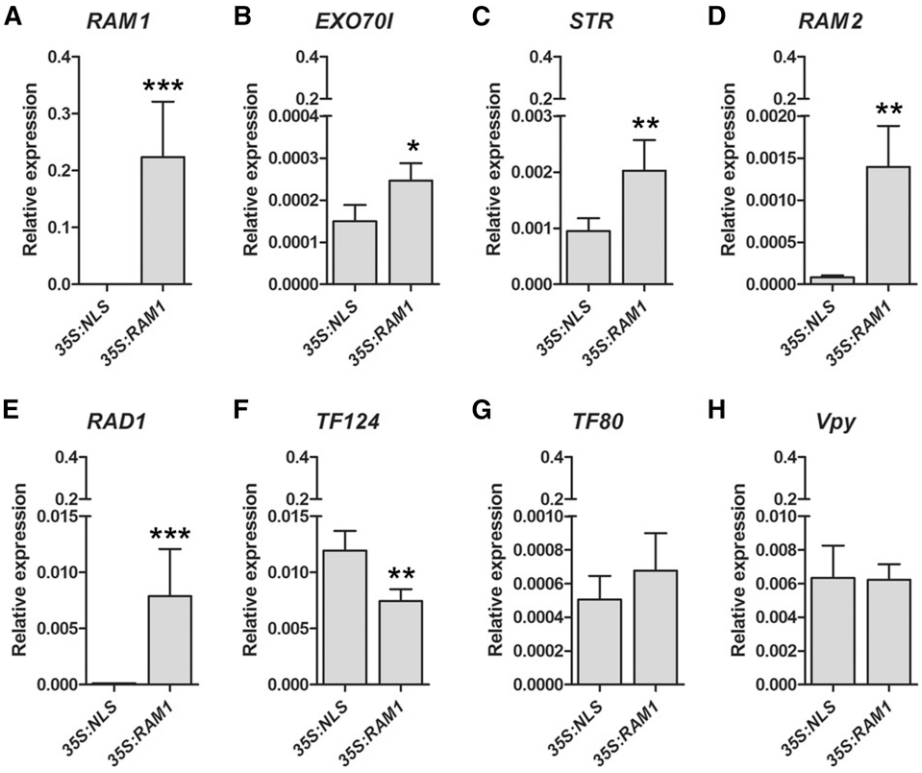

Figure 6. Ectopic overexpression of *RAM1* increases transcript levels of several genes involved in AM symbiosis. A to H, Relative expression of a selection of genes in wild-type (A17) roots expressing *35Spro:RAM1* (*35S:RAM1*) or a control construct *35Spro:NLS-GFP-GUS* (*35S:NLS*). The data are the means of three independent experiments, each with three to five biological replicates. The data were analyzed using a mixed effects model (Fit model on JMP Pro-10) with a fixed treatment effect and a random experiment effect on JMP Pro-10 ("Materials and Methods"). Error bars indicate SEM ($n \geq 10$). Asterisks indicate significant differences in transcript levels between *RAM1* overexpression plants and vector control plants. Expression is relative to *M. truncatula elongation factor1α*. *, $P < 0.05$; **, $P < 0.01$; ***, $P < 0.001$.

the *ram1-3* phenotype and the conclusion that *STR* and *EXO70I* are regulated by RAM1.

Yeast Two-Hybrid Analysis Detects Interactions between RAM1 and Several GRAS TFs

Previous studies indicate that some GRAS factors bind to DNA (Ma et al., 2014), whereas others are engaged with the promoter through a complex with other protein(s) (Fode et al., 2008; Hirsch et al., 2009). We failed to find evidence of direct binding of RAM1 to the *STR* and *EXO70I* promoters in either a yeast (*Saccharomyces cerevisiae*) one-hybrid assay or a *Nicotiana benthamiana* transactivation assay, and therefore, we used a targeted yeast two-hybrid analysis to identify additional potential interaction partners for RAM1 (Supplemental Fig. S9). As reported previously, we found that RAM1 interacts with the GRAS factor NSP2 (Gobbato et al., 2012) and also, GRAS factors RAD1 and TF80 (Medtr3g022830). The RAM1-RAD1 interaction is consistent with recent data from *L. japonicas*, where the *Lj*RAD1-*Lj*RAM1 interaction was shown in yeast and in planta (Xue et al., 2015). However, the interaction of RAM1 with TF80 has not been reported previously. Interactions between RAM1 and Medtr8g442410 (TF124), the third homolog in the RAM1 clade, could not be assayed because of autoactivation.

An *M. truncatula rad1* Mutant Shows Reduced Colonization

Because TF80 and RAD1 are potential interaction partners of RAM1, we searched for insertion mutants with which to further evaluate the roles of these proteins in symbiosis. A potential *TF80* insertion line is reported in the FST database (http://bioinfo4.noble.org/mutant/; NF14469), but the seed batch did not contain an insertion in *TF80*. However, we were able to obtain *M. truncatula* line NF9554 and verify a *Tnt1* insertion in *RAD1* located 75 nucleotides downstream of the start codon. The line was backcrossed, and colonization of the *rad1* mutant was compared with either R108 or a wild-type segregant from the backcrossed population. At 2 and 6 dpi, quantitative analysis of infection structures indicated no differences in the morphology of colonization in *rad1* relative to the wild-type segregant (Fig. 7A). However, at 3 wpp, colonization levels in *rad1* were slightly lower than those in the wild type, and this difference increased at 5 wpp (Fig. 7B). In addition, we examined colonization levels in *rad1* grown with slightly higher levels of P fertilization to determine whether the effects were robust and visible in more than one condition. In this experiment, differences in the levels of colonization were apparent only at 5 and 7 wpp but in both experiments, colonization levels in the wild type and wild-type segregant increased more rapidly than in *rad1* (Fig. 7, B and C). Based on these data, we suggest that intraradical colonization proceeds more slowly in *rad1* than in the wild type. Consistent with the colonization data at 3 wpp, *G. versiforme α-tubulin*, *PT4*, and *RAM1* transcript levels were similar in *rad1* and the wild type; however, *STR* transcripts were slightly lower in *rad1* relative to the wild type, suggesting that RAD1 might also contribute to the regulation of expression of this gene

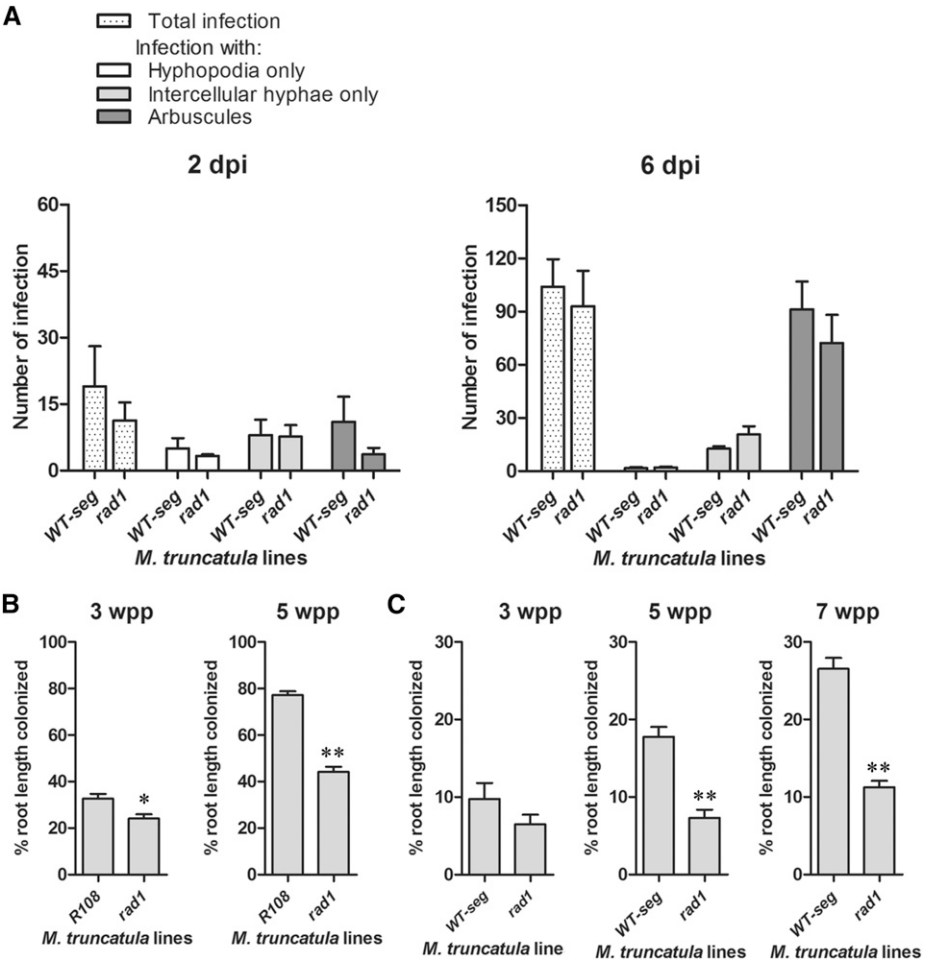

Figure 7. Colonization levels in *M. truncatula rad1*. A, Quantitation of total infection units, with hyphopodia only, infection units with intercellular hyphae only, and infection units with arbuscules in *rad1* and a wild-type segregant (WT-seg) from the *rad1* backcrossed population at 2 and 6 dpi with *G. versiforme* in a double-cone assay system. For each line, the data are the means of three biological replicate cones each containing two plants. B, The total percentage of colonized root length in *rad1* and R108 at 3 and 5 wpp with *G. versiforme*. Plants were fertilized with a modified one-half-strength Hoagland's solution with 20 μM phosphate. C, The total percentage of colonized root length in *rad1* and R108 at 3, 5, and 7 wpp with *G. versiforme*. Plants were fertilized with a modified one-half-strength Hoagland's solution with 200 μM phosphate. Error bars show SEM ($n \geq 3$). Asterisks indicate significant differences (Student's *t* test). *, $P < 0.05$; **, $P < 0.01$.

(Supplemental Fig. S10). However, in contrast to *RAM1*, overexpression of *RAD1* did not result in an increase in *STR* transcripts. Additionally, overexpression of *TF80* or *TF124* did not result in increases in *STR* transcripts (data not shown). Based on the phenotypes and gene expression data, it is possible that RAM1 interacts with RAD1 for activation of gene expression but that RAD1 function is partially redundant.

Overexpression of *della1-Δ18* Induces Expression of *RAM1*

RAM1 is necessary to enable arbuscule branching, and its expression is induced in colonized cortical cells. In *M. truncatula* and pea, DELLA proteins are also required to enable arbuscule development, and in *della* double mutants, AM fungi colonize the root cortex but fail to make arbuscules (Floss et al., 2013; Foo et al., 2013; Yu et al., 2014; Takeda et al., 2015). Because it is known that DELLAs act by regulating the expression of TFs or modulating their activity (Davière and Achard, 2013), we considered the possibility that DELLA1 regulates expression of RAM1. To evaluate this, we generated roots overexpressing a constitutively active DELLA protein (*della1-Δ18*; Floss et al., 2013) and analyzed expression of *RAM1* and a selection of other genes associated with arbuscule development. Constitutive expression of *della1-Δ18*, in mock-inoculated roots, was sufficient to result in small but significant increases in transcript levels of *RAM1* and *RAD1* but not *TF80* or *TF124*. Additionally, *RAM2*, *EXO70I*, and *STR* transcripts were also increased by *della1-Δ18* overexpression but to much lower levels than *RAM1* or *RAD1* (Fig. 8). Thus, DELLA1 promotes increases in RAM1 expression, and we speculated that increases in RAM1 subsequently led to increased expression of *RAM2*, *EXO70I*, and *STR*. To test this hypothesis, we overexpressed *della1-Δ18* in *ram1-1* and evaluated *RAM2*, *EXO70I*, and *STR* transcript levels. This revealed that *della1-Δ18*-induced increases in *RAM2*, *RAD1*, and *EXO70I* transcripts but not *STR* were dependent on RAM1 (Fig. 8, B–D). Because *STR* shows expression before symbiosis, it is likely that the basal expression is regulated differently than the symbiosis-induced expression. The observation that a *della1-Δ18*-induced increase in *STR* transcripts in colonized roots was RAM1 dependent supports this argument (data not shown). Taken together with the results of RAM1 overexpression (Fig. 6), we suggest that the

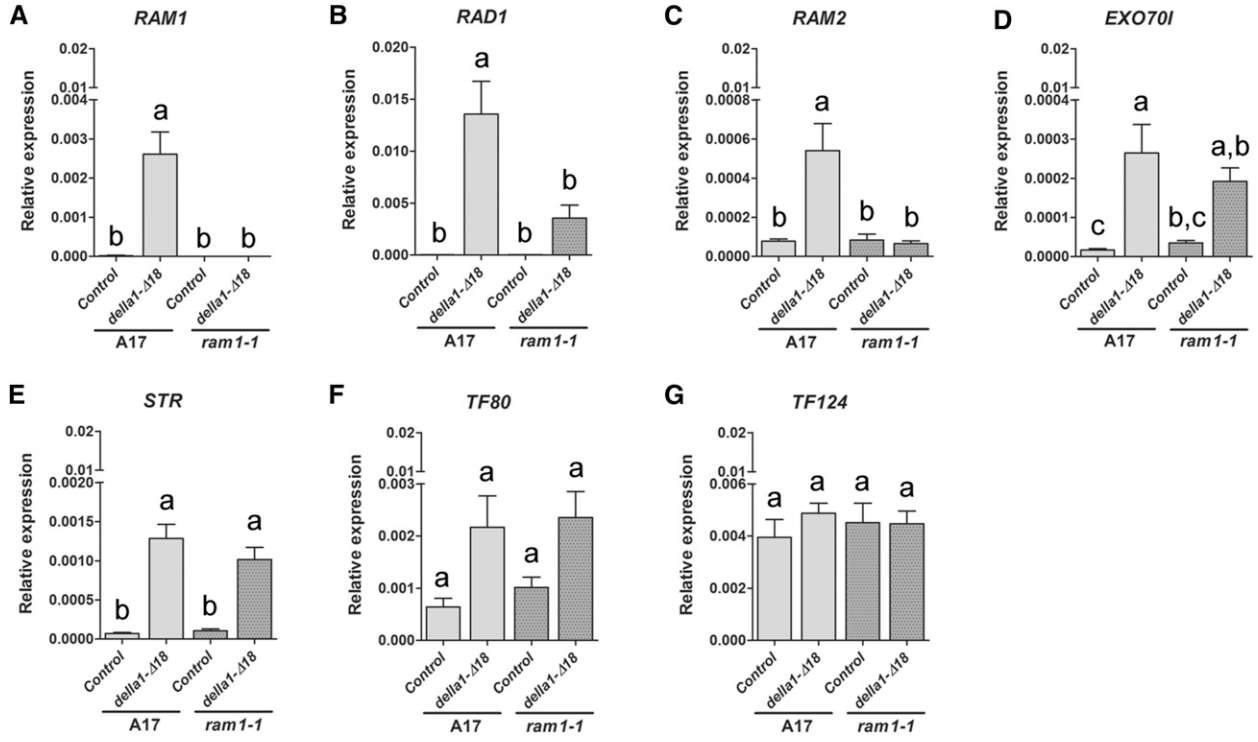

Figure 8. Overexpression of *della1-Δ18* increases *RAM1* transcripts. A to G, Relative expression of a selection of genes in A17 and *ram1-1* roots overexpressing a dominant *della* gene, *35Spro:della1-Δ18* (*della-Δ18*) or a *35Spro:GFP* vector control (Control). Error bars indicate SEM ($n \geq 4$). Different letters indicate significant transcript levels among *della1-Δ18* overexpression and vector control A17 or *ram1-1* roots differences (all pairs; Tukey's HSD mean-separation test; $P < 0.05$ in B; $P < 0.01$ in A and C–G). Gene expression is relative to *M. truncatula elongation factor1α*.

symbiosis-induced expression of *RAM2*, *RAD1*, *EXO70I*, and *STR* genes is regulated by RAM1 and that RAM1 expression is regulated by DELLA (Fig. 9).

DISCUSSION

Arbuscules are generally described as hyphae that have a tree-like structure, which includes a trunk from which thick branches and gradually finer branches arise. The periarbuscular membrane that surrounds the arbuscule is one continuous membrane, but its protein composition defines two large domains: a trunk domain, which surrounds the hyphal trunk and the first thick branches, and a branch domain, which encompasses the fine hyphal branches. Here, we provide evidence that RAM1 is essential to enable arbuscule branching and regulates expression of some genes associated with the branch domain of the periarbuscular membrane. In contrast to previous analyses, we do not find evidence that RAM1 is necessary to support hyphopodium formation, and it is possible that this interpretation arose from the late time points used for the original phenotypic analyses (Gobbato et al., 2012). In wild-type roots, a productive symbiosis results in secondary infection events, and at late time points, colonization levels are high. In contrast, at late time points, colonization levels in *ram1* are low because of the failing symbiosis, and it is possible that this was interpreted as a defect in entry into the root rather than a failure in cortical colonization and establishment of the symbiosis. Here, a detailed analysis of *ram1-3*, beginning at 48 h and extending to 5 weeks postinoculation, revealed that the fungal symbiont is capable of entering *ram1-3* roots and also, the cortical cells but that the hyphae fail to undergo the repeated dichotomous branching typical of an arbuscule in wild-type roots. Because RAM1 is a GRAS protein, it is reasonable to infer that it controls essential transcriptional events required specifically for the branching phase of arbuscule development. Furthermore, the *ram1-3* phenotype suggests that the cellular commitment to a program that supports arbuscule development occurs not at the point of hyphal penetration of the cortical cell but after the hypha has entered the cell. A transcriptional program coordinated with arbuscule branching also correlates with previous findings of membrane protein distribution in the periarbuscular membrane trunk and branch domains (Pumplin et al., 2012), and therefore, genes encoding membrane proteins of the branch domain are potential candidates for regulation by RAM1.

RAM1 is predicted to encode a transcriptional regulator of the GRAS family, and in previous studies of

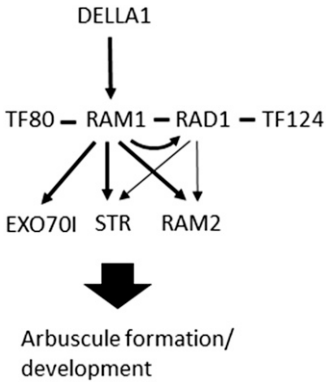

Figure 9. RAM1 regulates genes required to support arbuscule branching. DELLA1 increases expression of *RAM1*, and RAM1 regulates transcription of *EXO70I* and *STR* either directly or indirectly and may do so as a complex with RAD1. RAM1 interacts with two GRAS TFs, RAD1 and TF80 (thick lines). The expression of *STR* and *RAM2* is decreased in *rad1* mutant roots (thin arrow lines).

GRAS factors, a transcriptional approach that combined analysis of loss-of-function mutants and ectopic expression proved a viable way to predict downstream target genes (Levesque et al., 2006). Taking a similar approach, transcript analyses of *ram1-3* mycorrhizal roots and also, roots overexpressing *RAM1* predict that AM-induced expression of *STR*, *EXO70I*, *RAM2*, and *RAD1* is regulated, at least in part, by RAM1. We were unable to show direct binding of RAM1 to *EXO70I* or *STR* upstream regulatory sequences, but because GRAS factors typically work in complexes, it is possible that the RAM1 interaction occurs through a complex with other DNA binding proteins. RAD1 is one potential candidate because *STR* transcript levels show a small but significant reduction in *rad1*, and *EXO70I* transcripts show a similar trend. In *L. japonicus*, RAD1 and RAM1 interact when coexpressed in *N. benthamiana* cells (Xue et al., 2015), and here, we observed interaction of RAD1 and RAM1 in yeast two-hybrid assays. However, although an RAM1/RAD1 complex shows transcriptional activation activity in yeast, we did not find evidence for activation of *EXO70I* or *STR* promoters. Previously, RAM1 was shown to associate with the *RAM2* promoter through interaction with a second GRAS factor NSP2 (Gobbato et al., 2012), and our yeast two-hybrid assays point to an interaction of RAM1 with an additional GRAS factor, TF80. Consequently, RAM1 in association with one or more of these other factors might be needed to enable interaction with the *EXO70I* and *STR* promoters. Chromatin immunoprecipitation assays would help to address these questions, and we prepared epitope-tagged RAM1 to enable these analyses. However, the tagged RAM1 proteins did not fully complement the *ram1* mutants, and therefore, it will be necessary to pursue these studies in another way.

EXO70I and STR are both required to support arbuscule branching (Zhang et al., 2010; Gutjahr et al., 2012; Zhang et al., 2015): EXO70I for development of the branch domain of the periarbuscular membrane and STR for export of an unknown substrate across the periarbuscular membrane. In *exo70i* and *str* mutants, arbuscule development is arrested early in the branching process. These phenotypes are also consistent with the proposal that RAM1 regulates *EXO70I* and *STR* expression. However, neither the *exo70i* nor the *str* phenotype is as severe as that of *ram1-3*, which suggests that expression of other genes involved in early arbuscule branching is also regulated by RAM1. Large numbers of mycorrhiza-induced TFs were identified in transcriptome analyses (Hogekamp and Küster, 2013; Xue et al., 2015), and therefore, TFs other than RAM1 must also regulate gene expression during symbiosis. Expression of some of these TFs may be regulated by RAM1, and we provide initial evidence that RAM1 can induce expression of *RAD1*. Whether this results in a second wave of gene regulation associated with later phases of arbuscule development or possibly, arbuscule degeneration remains to be determined.

RAM1 itself shows strong transcriptional induction in mycorrhizal roots, specifically in the colonized regions of the root cortex. Therefore, we considered the question of what controls *RAM1* expression. It has been shown that DELLA proteins are essential for arbuscule development, but the TFs through which DELLAs act to promote arbuscule development have not been reported. Here, we show that ectopic expression of a dominant *della* gene increases *RAM1* and *RAD1* transcript levels but not *TF80* or *TF124*, the other two genes in the RAM1 clade. There are prior examples of DELLAs regulating transcription of other GRAS factors and also, GRAS factors that activate transcription of other GRAS factors, which we potentially see here with RAM1 and RAD1 (Levesque et al., 2006; Heo et al., 2011; Zhang et al., 2011). Additionally, some GRAS proteins bind to their own promoters and autoregulate their transcription (Cui et al., 2007; Zhang et al., 2011). Furthermore, a single GRAS factor can activate or repress gene expression depending on its interaction partner and in some cases, potentially through modification of heterochromatin (Cui and Benfey, 2009). Thus, there is much potential for complex regulation mediated by this class of TFs.

In conclusion, these data indicate that RAM1 regulates at least two genes required to enable arbuscule branching and also, increases expression of RAD1. Transcript levels of RAM1 are modulated by DELLA activity; thus, the data also provide information about the TFs through which DELLAs act to enable development of arbuscules (Fig. 9). Yeast two-hybrid data indicate potential interactions between these GRAS proteins, and future studies should focus on evaluating these complexes and their roles in regulating gene expression during AM symbiosis.

MATERIALS AND METHODS

Plant Growth and Inoculation with *Glomus versiforme*

Medicago truncatula wild-type or mutant seedlings or transformed plants were grown with *Glomus versiforme* in either cones or a double-cone system. The cones contained a mixture of gravel and sand with 100 or 150 *G. versiforme* spores positioned approximately 6 cm below the top of the gravel-sand mix in a 2- to 3-mm sand layer. Seedlings were transplanted into the cones and harvested at 3 to 5 wpp. The double-cone system was established as described previously (Lopez-Meyer and Harrison, 2006), and seedlings were transplanted into the upper cone and grown for 2 weeks before being placed over the lower cone containing 300 *G. versiforme* spores and grown together for an additional 9 d before pushing two cones together to establish contact between the germinated spores and root mat. Roots were harvested at 2, 4, 6, and 8 dpi. In this system, the inoculation day is known, hence the terminology dpi.

All plants were grown in a growth chamber in a 16-h/8-h and 25°C/22°C day-night cycle and fertilized with a modified one-half-strength Hoagland's nutrient solution containing 20 μM potassium phosphate twice a week (Javot et al., 2011) unless indicated otherwise.

For the experiment involving different nutrient treatments, *ram1-3* seedlings were transplanted into gravel-sand mix containing *G. versiforme* spores and fertilized with the above nutrient fertilizer for 1 week and then one-half-strength Hoagland's solution with 20 μM phosphate and 1.5 mM N, one-half-strength Hoagland's solution with 20 μM phosphate and 7.5 mM N, or one-half-strength Hoagland's solution with 20 mM phosphate and 7.5 mM N for another 3 weeks (Javot et al., 2011). The plants were harvested, and the roots were stained with Alexa Fluor 488 WGA (Molecular Probes) to allow visualization of the fungal structures (Hong et al., 2012).

Tnt1 Insertion Lines and Cosegregation Analysis

The *Tnt1* insertion mutant lines (*ram1-3*; NF5445 and *rad1*; NF9554) were identified from the *M. truncatula* mutant database (http://bioinfo4.noble.org/mutant/). Homozygous plants were identified by genotyping and crossed with the R108 wild type. The F1 generation was selfed, and homozygotes were identified from the F2. These homozygotes and also, wild-type segregants from the backcrossed population were used for experiments, except for the double-cone assays, in which homozygous plants before backcross were used.

For the genotype analysis, genomic DNA was extracted from an *M. truncatula* leaf as described (Dellaporta et al., 1983) with minor modifications. The leaf was frozen in liquid N and homogenized with two metal beads in a 2-mL tube. PCR-based genotyping was carried out with primers B2439/B2550 to detect the wild-type *RAM1* allele and B2439/B2377 for the *Tnt1* insertion in *RAM1*, B2548/B2549 for the wild-type *RAD1* allele, and B2548/B2501 for the Tnt1 insertion in *RAD1*. The primer sequences are shown in Supplemental Table S1.

For the cosegregation study, 120 segregating F2 plants were transplanted into cones (one plant per cone) containing *G. versiforme* spores, and both the genotype and phenotype were assessed.

Plasmid Construction

For the complementation tests, the *RAM1pro*:*RAM1* construct was created using MultiSite gateway cloning; 800 bp of DNA directly upstream of the first ATG of the *RAM1* gene was amplified by PCR with primers B3386 and B3387 from *M. truncatula* Jemalong A17 genomic DNA and cloned into pDONR P4-P1R (Invitrogen). The coding region of *RAM1* was amplified by PCR with primers B3249 and B3250 from *G. versiforme*-colonized root complementary DNA (cDNA) of *M. truncatula* A17 and cloned into pDONR221. pDONR4.1 *RAM1* promoter, pDONR221 *RAM1* coding sequence (CDS), pDONR2.3 Ubiquitin (UBQ) terminator (Ivanov and Harrison, 2014), and pKm43GW (Karimi et al., 2005) were mixed in a MultiSite gateway cloning reaction (Invitrogen), resulting in the *pRAM1*:*RAM1* binary vector.

To overexpress *RAM1*, *35Spro*:*RAM1* was generated from pDNOR221 *RAM1* CDS, pDONR4.1 35S promoter, pDONR2.3 35S terminator, and pK7m34GW-RR in a MultiSite gateway reaction. pK7m34GW-RR was created from K7m34GW (Karimi et al., 2005) by amplifying the *UBQ10pro*:*DsRED-NOSterm* from pRedRoot (Limpens et al., 2005) using primers B3701 and B3702 and ligating into the *Apa*I site in pK7m34GW (Karimi et al., 2005; S.Ivanov and M.J.Harrison, unpublished data).

For promoter analysis of *RAM1*, two constructs were generated. Two regions, 2 kb and 800 bp upstream of the first ATG of the *RAM1* gene, were amplified by PCR with primers B3842, B3843, and B3844, digested with *Kpn*I and *Pst*I, and then ligated into pCAMBIA2301-Δ35S promoter (Pumplin et al., 2010) to create *RAM1pro2kb*:*UidA* and *RAM1pro800*:*UidA*.

For yeast (*Saccharomyces cerevisiae*) assays, pEG202-SC and pJG4-5-SC plasmids containing SMART III and CDS III (SC) sequences were created. The SC sequences were amplified from pGADT7-Rec2 (Clontech) using the primers B1881/B1882 with *Eco*RI/*Sma*I sites and B1883/B1884 with *Sma*I/*Xho*I sites for pJG4-5 and B1905/B1906 with *Eco*RI/*Pml*I sites and B1907/B1908 with *Pml*I/*Xho*I sites for pEG202 and cloned into pEG202 to create a binding domain fusion plasmid and pJG4-5 for an activation domain (*LexA Repressor*) fusion plasmid. pEG202-SC digested with *Pml*I or pJG4-5-SC digested with *Sma*I was mixed with *RAD1*, *RAM1*, and *NSP2* coding sequences amplified from *M. truncatula* cDNA (primers described in Supplemental Table S1) to generate binding domain-fusion and activation domain-fusion plasmids, which were then transformed into yeast strains EGY48 or Y864. To construct pEG202-GW and pJG4-5-GW, a gateway sequence (GW) was amplified from pDEST22 (Invitrogen) using the primers B3757 with *Eco*RI and B3758 with *Xho*I and cloned into the multiple cloning site of each plasmid. pEG202-GW or pJG4-5-GW was mixed with coding sequences (*TF80* and *TF124*) amplified from *M. truncatula* cDNA (using primers described in Supplemental Table S1) to create binding domain-fusion and activation domain-fusion plasmids.

Agrobacterium rhizogenes-Mediated Transformation of *M. truncatula* Roots

M. truncatula root transformation was performed as described in Boisson-Dernier et al. (2001) with slight modifications as follows: the cut ends of *M. truncatula* (A17, R108, or mutants) seedling roots were cocultivated with *Agrobacterium rhizogenes* containing a binary vector. After cocultivation, the plants with transformed roots were transplanted in Turface (Profile Products) and grown for 10 d to allow more root growth. The plants were then transplanted to cones with 100 to 150 spores of *G. versiforme* and grown for 3 to 7 weeks as described above.

Staining Roots with Alexa Fluor 488 WGA and Propidium Iodide and Quantification of Colonization

Roots were fixed with 50% (v/v) ethanol for 4 h, cleared in 20% (v/v) potassium hydroxide solution for 4 d at room temperature, rinsed thoroughly with distilled water, and then incubated with 0.2 μg mL^{-1} Alexa Fluor 488 WGA in phosphate-buffered saline for 1 d in the dark. In some instances, roots were incubated in propidium iodide (20 μg mL^{-1} in distilled water) to stain the cell wall. Stained roots were examined microscopically using either a fluorescence stereomicroscope or a confocal microscope. For infection unit analysis of *ram1-3* grown in the double cones and harvested at 2, 4, and 6 dpi, all colonization events (hyphopodia, intercellular hyphae, arbuscules, trunks, and undeveloped arbuscules) on the root systems of plants grown in the double cones were counted. At the 8-dpi, 3-wpp, and 5-wpp time points, the percentage of infected root pieces containing hyphopodia, intercellular hyphae, arbuscules, or arbuscule trunks/undeveloped arbuscules was scored using the modified gridline intersect method (McGonigle et al., 1990).

RNA Isolation, Semi-qRT-PCR, and qRT-PCR

Total RNA was extracted from roots with TRIzol reagent according to the manufacturer's instruction manual (www.lifetechnologies.com). cDNA was synthesized using SuperScript III Reverse Transcriptase (Invitrogen) from 500 ng of total RNA. The cDNA equivalent of 10 ng of RNA was used for semi-qRT-PCR and real-time qRT-PCR.

Histochemical GUS Staining

For GUS staining of *M. truncatula* roots transformed with *RAM1pro2kb*:*UidA* and *RAM1pro800*:*UidA*, the plant roots were harvested at 3 and 5 wpp and incubated in GUS staining buffer (0.5 mg mL^{-1} 5-bromo-4-chloro-3-indolyl-β-D-glucuronide cyclohexylammonium salts, 100 mM NaH_2PO_4, pH 7.0, and 5 mM Na_2EDTA) for 2 to 4 h at 37°C and then fixed with fixation buffer of 50 mM PIPES, pH 6.9, 5 mM $MgSO_4$, 50 mM EGTA, 11% (v/v) formaldehyde, and 5% (v/v) dimethyl sulfoxide for 1 d (Liu et al., 2008) before clearing with potassium hydroxide and staining with Alexa Fluor 488 WGA as outlined above.

P Content Analyses

The phosphate content of the shoots of *M. truncatula* plants grown under three different nutrient regimes was measured to confirm the nutrient treatment in Figure 4. Leaf tissue was ground in liquid N, and the soluble phosphate content was measured as described (Ames, 1966).

The data are as follows: 20 μM inorganic phosphate (Pi): 1.5 mM N-R108 (22.04 ± 3.71 [mean ± SD; nanomoles Pi per milligram dry weight]); 20 μM Pi: 1.5 mM N-wild-type-seg (25.19 ± 5.76 [mean ± SD; nanomoles Pi per milligram dry weight]); 20 μM Pi: 1.5 mM *N-ram1-3* (25.29 ± 1.07 [mean ± SD; nanomoles Pi per milligram dry weight]); 20 μM Pi: 7.5 mM N-R108 (21.73 ± 5.59 [mean ± SD; nanomoles Pi per milligram dry weight]); 20 μM Pi: 7.5 mM N-wild-type-seg (19.49 ± 0.89 [mean ± SD; nanomoles Pi per milligram dry weight]); 20 μM Pi: 7.5 mM *N-ram1-3* (21.74 ± 1.89 [mean ± SD; nanomoles Pi per milligram dry weight]); 2 mM Pi: 7.5 mM N-B108 (258.95 ± 9.69 [mean ± SD; nanomoles Pi per milligram dry weight]); 2 mM Pi: 7.5 mM N-wild-type-seg (251.90 ± 37.03 [mean ± SD; nanomoles Pi per milligram dry weight]); and 2 mM Pi: 7.5 mM *N-ram1-3* (171.41 ± 28.64 [mean ± SD; nanomoles Pi per milligram dry weight]).

Shoot phosphate level of the *M. truncatula* plants fertilized with high-Pi fertilizer (2 mM Pi and 7.5 mM N) showed a significant increase compared with those fertilized with two low-Pi fertilizers.

Yeast Two-Hybrid Assay

For yeast two-hybrid assays, plasmids containing the DNA-binding domain fusion *TF* genes were transformed into yeast strain EGY48 containing the *LacZ* (β-galactosidase) reporter (pSH18-34). The plasmids of LexA fusion *TF* genes were transformed into strain Y864. The two yeast strains were mated, resulting in yeast containing the three plasmids. The mated yeasts were grown on the dropout (SD-Ura-Trp-His) plates containing 5-bromo-4-chloro-3-indolyl-β-D-galactopyranoside for color development (Zeng et al., 2012).

Statistical Analysis

The measured data were analyzed by Student's *t* test or pairwise comparison using all pairs Tukey's honestly significant difference (HSD) mean-separation test on JMP Pro-10 software. The statistical information, including numbers of biological replicates, means, and error bars, is described in each figure legend. To analyze variances between genotypes and nutrient treatments groups in Figure 4B, the experimental data were analyzed using ANOVA test on JMP Pro-10. To determine if there was a significant effect of *RAM1* overexpression in Figure 6, data from three independent experiments were analyzed together. The expression data for each candidate target gene were right skewed so a natural log transformation was applied before analysis. The transformed expression data were analyzed using a linear mixed model with a fixed treatment effect and a random experiment effect. *F* tests were used to determine whether there was a significant treatment effect. All statistical analyses were performed using the JMP statistical software package (JMP, version 10; SAS Institute Inc., Cary, NC).

Phylogenetic Analysis

The predicted full-length amino acid sequences of all GRAS TFs were obtained by iteratively blasting the TF RAM1 (Medtr7g027190) in a database containing the predicted protein models from the genomes of Arabidopsis (*Arabidopsis thaliana*; TAIR), rice (*Oryza sativa*; phytozome10), *Lotus japonicus* (Kazusa DNA Research Institute), and *M. truncatula* (JCVI). The protein models were aligned using the program MAFFT, version 7.205, with default values, and the columns containing more than 50% of gaps were eliminated from the alignment. The approximately maximum likelihood phylogenetic tree was generated using FastTree, version 2.1.5, with the wag model of amino acid evolution. Two TFs that are closely related to GRAS factors were used to root the tree. Each branch division shows local support values with the Shimodaira-Hasegawa test (Price et al., 2010).

Supplemental Data

The following supplemental materials are available.

Supplemental Figure S1. *RAM1* is expressed in the root cortex in regions that are colonized and can also be detected in younger regions of some lateral roots in both mock-inoculated and colonized root systems.

Supplemental Figure S2. Diagram showing the sites of *Tnt1* insertions in the *RAM1* gene.

Supplemental Figure S3. Confocal microscope images showing the mycorrhizal phenotype of *ram1-3* at 4 and 8 dpi with *G. versiforme* in the double-cone system.

Supplemental Figure S4. Mycorrhizal colonization phenotype of *ram1-3* plants colonized with *G. versiforme* at 4 and 8 dpi.

Supplemental Figure S5. A comparison of colonization in *ram1-1* and *ram1-3*.

Supplemental Figure S6. *ram1-3* complementation and cosegregation analysis.

Supplemental Figure S7. Phylogenetic tree of GRAS TFs.

Supplemental Figure S8. Gene expression in *ram1-1*.

Supplemental Figure S9. Yeast two-hybrid assays to assess the interaction of various TFs and regulators.

Supplemental Figure S10. Gene expression in *rad1*.

Supplemental Table S1. List of primers and genes.

Supplemental Data Set S1. GRAS family alignment file.

ACKNOWLEDGMENTS

We thank Lynn Marie Johnson (Cornell Statistical Consulting Unit, Cornell University) for helping with the statistical analysis of gene expression in roots overexpressing RAM1.

Received July 23, 2015; accepted October 28, 2015; published October 28, 2015.

LITERATURE CITED

Akiyama K, Matsuzaki K, Hayashi H (2005) Plant sesquiterpenes induce hyphal branching in arbuscular mycorrhizal fungi. Nature **435:** 824–827

Ames BN (1966) Assay of inorganic phosphate, total phosphate and phosphatases. Methods Enzymol **8:** 115–118

Amijee F, Tinker PB, Stribley DP (1989) The development of endomycorrhizal root systems. VII. A detailed study of effects of soil phosphorus on colonization. New Phytol **111:** 435–446

Baath E, Spokes J (1989) The effect of added nitrogen and phosphorus on mycorrhizal growth response and infection in *Allium schoenoprasum*. Can J Bot **67:** 3227–3232

Besserer A, Puech-Pagès V, Kiefer P, Gomez-Roldan V, Jauneau A, Roy S, Portais JC, Roux C, Bécard G, Séjalon-Delmas N (2006) Strigolactones stimulate arbuscular mycorrhizal fungi by activating mitochondria. PLoS Biol **4:** e226

Boisson-Dernier A, Chabaud M, Garcia F, Becard G, Rosenberg C, Barker DG (2001) *Agrobacterium* rhizogenes-transformed roots of *Medicago truncatula* for the study of nitrogen-fixing and endomycorrhizal symbiotic associations. Mol Plant Microbe Interact **14:** 695–700

Bolle C (2004) The role of GRAS proteins in plant signal transduction and development. Planta **218:** 683–692

Breuillin-Sessoms F, Floss DS, Gomez SK, Pumplin N, Ding Y, Levesque-Tremblay V, Noar RD, Daniels DA, Bravo A, Eaglesham JA, et al (2015) Suppression of arbuscule degeneration in *Medicago truncatula phosphate transporter4* mutants is dependent on the Ammonium Transporter 2 family protein AMT2;3. Plant Cell **27:** 1352–1366

Cui H, Benfey PN (2009) Interplay between SCARECROW, GA and LIKE HETEROCHROMATIN PROTEIN 1 in ground tissue patterning in the Arabidopsis root. Plant J **58:** 1016–1027

Cui H, Levesque MP, Vernoux T, Jung JW, Paquette AJ, Gallagher KL, Wang JY, Blilou I, Scheres B, Benfey PN (2007) An evolutionarily conserved mechanism delimiting SHR movement defines a single layer of endodermis in plants. Science **316:** 421–425

Davière JM, Achard P (2013) Gibberellin signaling in plants. Development **140:** 1147–1151

Delaux PM, Bécard G, Combier JP (2013) NSP1 is a component of the Myc signaling pathway. New Phytol **199:** 59–65

Dellaporta SL, Wood J, Hicks JB (1983) A plant DNA minipreparation. Plant Mol Biol Report **1:** 19–22

Devers EA, Branscheid A, May P, Krajinski F (2011) Stars and symbiosis: microRNA- and microRNA*-mediated transcript cleavage involved in arbuscular mycorrhizal symbiosis. Plant Physiol **156:** 1990–2010

Devers EA, Teply J, Reinert A, Gaude N, Krajinski F (2013) An endogenous artificial microRNA system for unraveling the function of root endosymbioses related genes in Medicago truncatula. BMC Plant Biol **13:** 82

Feddermann N, Muni RRD, Zeier T, Stuurman J, Ercolin F, Schorderet M, Reinhardt D (2010) The PAM1 gene of petunia, required for intracellular accommodation and morphogenesis of arbuscular mycorrhizal fungi, encodes a homologue of VAPYRIN. Plant J **64:** 470–481

Floss DS, Levy JG, Levesque-Tremblay V, Pumplin N, Harrison MJ (2013) DELLA proteins regulate arbuscule formation in arbuscular mycorrhizal symbiosis. Proc Natl Acad Sci U S A **110:** E5025–E5034

Fode B, Siemsen T, Thurow C, Weigel R, Gatz C (2008) The *Arabidopsis* GRAS protein SCL14 interacts with class II TGA transcription factors and is essential for the activation of stress-inducible promoters. Plant Cell **20:** 3122–3135

Foo E, Ross JJ, Jones WT, Reid JB (2013) Plant hormones in arbuscular mycorrhizal symbioses: an emerging role for gibberellins. Ann Bot (Lond) **111:** 769–779

Frenzel A, Manthey K, Perlick AM, Meyer F, Pühler A, Küster H, Krajinski F (2005) Combined transcriptome profiling reveals a novel family of arbuscular mycorrhizal-specific *Medicago truncatula* lectin genes. Mol Plant Microbe Interact **18:** 771–782

Gaude N, Bortfeld S, Duensing N, Lohse M, Krajinski F (2012) Arbuscule-containing and non-colonized cortical cells of mycorrhizal roots undergo extensive and specific reprogramming during arbuscular mycorrhizal development. Plant J **69:** 510–528

Genre A, Chabaud M, Balzergue C, Puech-Pagès V, Novero M, Rey T, Fournier J, Rochange S, Bécard G, Bonfante P, et al (2013) Short-chain chitin oligomers from arbuscular mycorrhizal fungi trigger nuclear Ca2+ spiking in Medicago truncatula roots and their production is enhanced by strigolactone. New Phytol **198:** 190–202

Gobbato E, Marsh JF, Vernié T, Wang E, Maillet F, Kim J, Miller JB, Sun J, Bano SA, Ratet P, et al (2012) A GRAS-type transcription factor with a specific function in mycorrhizal signaling. Curr Biol **22:** 2236–2241

Gobbato E, Wang E, Higgins G, Bano SA, Henry C, Schultze M, Oldroyd GED (2013) RAM1 and RAM2 function and expression during arbuscular mycorrhizal symbiosis and Aphanomyces euteiches colonization. Plant Signal Behav **8:** e26049

Gutjahr C, Radovanovic D, Geoffroy J, Zhang Q, Siegler H, Chiapello M, Casieri L, An K, An G, Guiderdoni E, et al (2012) The half-size ABC transporters STR1 and STR2 are indispensable for mycorrhizal arbuscule formation in rice. Plant J **69:** 906–920

Harrison MJ, Dewbre GR, Liu J (2002) A phosphate transporter from *Medicago truncatula* involved in the acquisition of phosphate released by arbuscular mycorrhizal fungi. Plant Cell **14:** 2413–2429

Heo JO, Chang KS, Kim IA, Lee MH, Lee SA, Song SK, Lee MM, Lim J (2011) Funneling of gibberellin signaling by the GRAS transcription regulator scarecrow-like 3 in the Arabidopsis root. Proc Natl Acad Sci USA **108:** 2166–2171

Hirsch S, Kim J, Muñoz A, Heckmann AB, Downie JA, Oldroyd GED (2009) GRAS proteins form a DNA binding complex to induce gene expression during nodulation signaling in *Medicago truncatula*. Plant Cell **21:** 545–557

Hofferek V, Mendrinna A, Gaude N, Krajinski F, Devers EA (2014) MiR171h restricts root symbioses and shows like its target NSP2 a complex transcriptional regulation in Medicago truncatula. BMC Plant Biol **14:** 199

Hogekamp C, Küster H (2013) A roadmap of cell-type specific gene expression during sequential stages of the arbuscular mycorrhiza symbiosis. BMC Genomics **14:** 306

Hohnjec N, Vieweg MF, Pühler A, Becker A, Küster H (2005) Overlaps in the transcriptional profiles of *Medicago truncatula* roots inoculated with two different Glomus fungi provide insights into the genetic program activated during arbuscular mycorrhiza. Plant Physiol **137:** 1283–1301

Hong JJ, Park YS, Bravo A, Bhattarai KK, Daniels DA, Harrison MJ (2012) Diversity of morphology and function in arbuscular mycorrhizal symbioses in Brachypodium distachyon. Planta **236:** 851–865

Ivanov S, Fedorova EE, Limpens E, De Mita S, Genre A, Bonfante P, Bisseling T (2012) Rhizobium-legume symbiosis shares an exocytotic pathway required for arbuscule formation. Proc Natl Acad Sci USA **109:** 8316–8321

Ivanov S, Harrison MJ (2014) A set of fluorescent protein-based markers expressed from constitutive and arbuscular mycorrhiza-inducible promoters to label organelles, membranes and cytoskeletal elements in Medicago truncatula. Plant J **80:** 1151–1163

Javot H, Penmetsa RV, Breuillin F, Bhattarai KK, Noar RD, Gomez SK, Zhang Q, Cook DR, Harrison MJ (2011) *Medicago truncatula mtpt4* mutants reveal a role for nitrogen in the regulation of arbuscule degeneration in arbuscular mycorrhizal symbiosis. Plant J **68:** 954–965

Javot H, Penmetsa RV, Terzaghi N, Cook DR, Harrison MJ (2007) A *Medicago truncatula* phosphate transporter indispensable for the arbuscular mycorrhizal symbiosis. Proc Natl Acad Sci USA **104:** 1720–1725

Karimi M, De Meyer B, Hilson P (2005) Modular cloning in plant cells. Trends Plant Sci **10:** 103–105

Koide R, Li M (1990) On host regulation of the vesicular-arbuscular mycorrhizal symbiosis. New Phytol **114:** 59–74

Krajinski F, Courty PE, Sieh D, Franken P, Zhang H, Bucher M, Gerlach N, Kryvoruchko I, Zoeller D, Udvardi M, et al (2014) The H+-ATPase HA1 of *Medicago truncatula* is essential for phosphate transport and plant growth during arbuscular mycorrhizal symbiosis. Plant Cell **26:** 1808–1817

Kretzschmar T, Kohlen W, Sasse J, Borghi L, Schlegel M, Bachelier JB, Reinhardt D, Bours R, Bouwmeester HJ, Martinoia E (2012) A petunia ABC protein controls strigolactone-dependent symbiotic signalling and branching. Nature **483:** 341–344

Levesque MP, Vernoux T, Busch W, Cui H, Wang JY, Blilou I, Hassan H, Nakajima K, Matsumoto N, Lohmann JU, et al (2006) Whole-genome analysis of the SHORT-ROOT developmental pathway in Arabidopsis. PLoS Biol **4:** e143

Limpens E, Mirabella R, Fedorova E, Franken C, Franssen H, Bisseling T, Geurts R (2005) Formation of organelle-like N2-fixing symbiosomes in legume root nodules is controlled by DMI2. Proc Natl Acad Sci USA **102:** 10375–10380

Liu J, Blaylock LA, Endre G, Cho J, Town CD, VandenBosch KA, Harrison MJ (2003) Transcript profiling coupled with spatial expression analyses reveals genes involved in distinct developmental stages of an arbuscular mycorrhizal symbiosis. Plant Cell **15:** 2106–2123

Liu J, Versaw WK, Pumplin N, Gomez SK, Blaylock LA, Harrison MJ (2008) Closely related members of the Medicago truncatula PHT1 phosphate transporter gene family encode phosphate transporters with distinct biochemical activities. J Biol Chem **283:** 24673–24681

Liu W, Kohlen W, Lillo A, Op den Camp R, Ivanov S, Hartog M, Limpens E, Jamil M, Smaczniak C, Kaufmann K, et al (2011) Strigolactone biosynthesis in *Medicago truncatula* and rice requires the symbiotic GRAS-type transcription factors NSP1 and NSP2. Plant Cell **23:** 3853–3865

Lopez-Meyer M, Harrison MJ (2006) An experimental system to synchronize the early events of development of the arbuscular mycorrhizal symbiosis. *In* F Sánchez, C Quinto, IM López-Lara, O Geiger, eds, Biology of Molecular Plant-Microbe Interactions, **Vol 5**. International Society for Molecular Plant Microbe Interactions, St. Paul, pp 546–551

Ma Z, Hu X, Cai W, Huang W, Zhou X, Luo Q, Yang H, Wang J, Huang J (2014) Arabidopsis miR171-targeted scarecrow-like proteins bind to GT cis-elements and mediate gibberellin-regulated chlorophyll biosynthesis under light conditions. PLoS Genet **10:** e1004519

Maillet F, Poinsot V, André O, Puech-Pagès V, Haouy A, Gueunier M, Cromer L, Giraudet D, Formey D, Niebel A, et al (2011) Fungal lipochitooligosaccharide symbiotic signals in arbuscular mycorrhiza. Nature **469:** 58–63

McGonigle TP, Miller MH, Evans DG, Fairchild GL, Swan JA (1990) A new method that gives an objective measure of colonization of roots by vesicular-arbuscular mycorrhizal fungi. New Phytol **115:** 495–501

Murray JD, Muni RRD, Torres-Jerez I, Tang Y, Allen S, Andriankaja M, Li G, Laxmi A, Cheng X, Wen J, et al (2011) Vapyrin, a gene essential for intracellular progression of arbuscular mycorrhizal symbiosis, is also essential for infection by rhizobia in the nodule symbiosis of Medicago truncatula. Plant J **65:** 244–252

Oldroyd GED (2013) Speak, friend, and enter: signalling systems that promote beneficial symbiotic associations in plants. Nat Rev Microbiol **11:** 252–263

Price MN, Dehal PS, Arkin AP (2010) FastTree 2: approximately maximum-likelihood trees for large alignments. PLoS One **5:** e9490

Pumplin N, Harrison MJ (2009) Live-cell imaging reveals periarbuscular membrane domains and organelle location in *Medicago truncatula* roots during arbuscular mycorrhizal symbiosis. Plant Physiol **151:** 809–819

Pumplin N, Mondo SJ, Topp S, Starker CG, Gantt JS, Harrison MJ (2010) Medicago truncatula Vapyrin is a novel protein required for arbuscular mycorrhizal symbiosis. Plant J **61:** 482–494

Pumplin N, Zhang X, Noar RD, Harrison MJ (2012) Polar localization of a symbiosis-specific phosphate transporter is mediated by a transient reorientation of secretion. Proc Natl Acad Sci USA **109:** E665–E672

Rech SS, Heidt S, Requena N (2013) A tandem Kunitz protease inhibitor (KPI106)-serine carboxypeptidase (SCP1) controls mycorrhiza establishment and arbuscule development in Medicago truncatula. Plant J **75:** 711–725

Rich MK, Schorderet M, Bapaume L, Falquet L, Morel P, Vandenbussche M, Reinhardt D (2015) A petunia GRAS transcription factor controls symbiotic gene expression and fungal morphogenesis in arbuscular mycorrhiza. Plant Physiol **168:** 788–797

Schwab SM, Menge JA, Leonard RT (1983) Quantitative and qualitative effects of phosphorus on extracts and exudates of sudangrass roots in relation to vesicular-arbuscular mycorrhiza formation. Plant Physiol **73:** 761–765

Singh S, Katzer K, Lambert J, Cerri M, Parniske M (2014) CYCLOPS, a DNA-binding transcriptional activator, orchestrates symbiotic root nodule development. Cell Host Microbe **15:** 139–152

Smith SE, Read DJ (2008) Mycorrhizal Symbiosis. Academic Press, Inc., San Diego

Smith SE, Smith FA (2011) Roles of arbuscular mycorrhizas in plant nutrition and growth: New paradigms from cellular to ecosystem scales. *In* SS Merchant, WR Briggs, D Ort, eds, Annual Review of Plant Biology, **Vol 62**. Annual Reviews, Palo Alto, CA, pp 227–250

Takeda N, Handa Y, Tsuzuki S, Kojima M, Sakakibara H, Kawaguchi M (2015) Gibberellins interfere with symbiosis signaling and gene expression and alter colonization by arbuscular mycorrhizal fungi in *Lotus japonicus*. Plant Physiol **167:** 545–557

Takeda N, Sato S, Asamizu E, Tabata S, Parniske M (2009) Apoplastic plant subtilases support arbuscular mycorrhiza development in Lotus japonicus. Plant J **58:** 766–777

Wang E, Schornack S, Marsh JF, Gobbato E, Schwessinger B, Eastmond P, Schultze M, Kamoun S, Oldroyd GED (2012) A common signaling process that promotes mycorrhizal and oomycete colonization of plants. Curr Biol **22:** 2242–2246

Wang E, Yu N, Bano SA, Liu C, Miller AJ, Cousins D, Zhang X, Ratet P, Tadege M, Mysore KS, et al (2014) A H+-ATPase that energizes nutrient uptake during mycorrhizal symbioses in rice and *Medicago truncatula*. Plant Cell **26:** 1818–1830

Xie X, Huang W, Liu F, Tang N, Liu Y, Lin H, Zhao B (2013) Functional analysis of the novel mycorrhiza-specific phosphate transporter AsPT1 and PHT1 family from Astragalus sinicus during the arbuscular mycorrhizal symbiosis. New Phytol **198:** 836–852

Xue L, Cui H, Buer B, Vijayakumar V, Delaux PM, Junkermann S, Bucher M (2015) Network of GRAS transcription factors involved in the control of arbuscule development in *Lotus japonicus*. Plant Physiol **167:** 854–871

Yang SY, Grønlund M, Jakobsen I, Grotemeyer MS, Rentsch D, Miyao A, Hirochika H, Kumar CS, Sundaresan V, Salamin N, et al (2012) Nonredundant regulation of rice arbuscular mycorrhizal symbiosis by two members of the *PHOSPHATE TRANSPORTER1* gene family. Plant Cell **24:** 4236–4251

Yano K, Yoshida S, Müller J, Singh S, Banba M, Vickers K, Markmann K, White C, Schuller B, Sato S, et al (2008) CYCLOPS, a mediator of symbiotic intracellular accommodation. Proc Natl Acad Sci USA **105:** 20540–20545

Yu N, Luo D, Zhang X, Liu J, Wang W, Jin Y, Dong W, Liu J, Liu H, Yang W, et al (2014) A DELLA protein complex controls the arbuscular mycorrhizal symbiosis in plants. Cell Res **24:** 130–133

Zeng L, Velásquez AC, Munkvold KR, Zhang J, Martin GB (2012) A tomato LysM receptor-like kinase promotes immunity and its kinase activity is inhibited by AvrPtoB. Plant J **69:** 92–103

Zhang Q, Blaylock LA, Harrison MJ (2010) Two *Medicago truncatula* half-ABC transporters are essential for arbuscule development in arbuscular mycorrhizal symbiosis. Plant Cell **22:** 1483–1497

Zhang X, Pumplin N, Ivanov S, Harrison MJ (2015) EXO70I is required for development of a sub-domain of the periarbuscular membrane during arbuscular mycorrhizal symbiosis. Curr Biol **25:** 2189–2195

Zhang ZL, Ogawa M, Fleet CM, Zentella R, Hu J, Heo JO, Lim J, Kamiya Y, Yamaguchi S, Sun TP (2011) Scarecrow-like 3 promotes gibberellin signaling by antagonizing master growth repressor DELLA in Arabidopsis. Proc Natl Acad Sci USA **108:** 2160–2165